



## Analysis of vehicle skidding potential on horizontal curves

Jia Peng<sup>a</sup>, L. Chu<sup>b</sup>, Tangjie Wang<sup>a</sup>, T.F. Fwa<sup>b,c,\*</sup>

<sup>a</sup> School of Highway, Chang'an University, Xi'an, China

<sup>b</sup> School of Highway, Chang'an University, China

<sup>c</sup> National University of Singapore, Singapore



### ARTICLE INFO

**Keywords:**

Horizontal curve  
Crashes  
Skidding mode  
Roadway departure  
Lane departure  
Pavement skid resistance

### ABSTRACT

High crash rates on horizontal curves during wet weather are a major road safety concern. Among the various causes of crashes on horizontal curves, wet-weather skidding is a major contributing factor. This study analyzed the mechanisms of three possible modes of vehicle skidding on horizontal curves based on theories of mechanics. The three modes of skidding analyzed were: (i) forward skidding of front steering wheel, (ii) sideway skidding of front steering wheel, and (iii) sideway skidding of rear wheel. The main objective was to provide useful information to researchers and practitioners in identifying the important factors that contribute to horizontal curve crashes. A computer simulation procedure was developed to evaluate the maximum safe vehicle speeds against the three modes of skidding on wet horizontal curved pavements. This offers a much improved method for skidding potential evaluation compared to the conventional approximate method using estimated coefficient of friction. The skidding potential of a vehicle is defined as the difference between its speed and the maximum safe speed against skidding. The smaller the difference, the higher is the skidding potential. The relative magnitudes of skidding potential for the three skidding modes were considered for different operating conditions. Different operating conditions were represented by different values of pavement curve radii, super-elevations, and wet-weather conditions represented by the thickness of pavement surface water-film. The analysis identified five key factors that affect the skidding potential of vehicles negotiating a horizontal curve. They are: vehicle speed, curve radius, superelevation, water film thickness and pavement skid resistance state.

### 1. Introduction

Horizontal curves have long been recognized to be among those road locations most vulnerable to crash occurrence. For instance, in the United States, the Federal Highway Administration stated in 2019 (FHWA, 2019) that “the average crash rate for horizontal curves is about three times that of other types of highway segments” and “more than 25 percent of fatal crashes are associated with a horizontal curve”. Therefore, it is not surprising that this issue has received much attention by researchers and highway agencies since 1970s (Taylor et al., 1972; Stimpson et al., 1977; Olsen, 1978). There have since been continuing efforts by researchers to reduce fatality and injury rates of crashes on horizontal curves (Glennon et al., 1985; Torbic et al., 2004; Donnell et al., 2019).

This study focuses on the possible modes of skidding on wet horizontal curves. Skidding occurs in a sudden unexpected manner. Caught by surprise, most drivers could not react correctly to prevent their vehicles from moving off the intended path of travel. Crash statistics from

literature suggest that this would be a worthwhile research undertaking. For example, FHWA (2020) reported that in the period from 2016 to 2018, lane and roadway departures contributed 51 percent of all traffic fatalities in the United States. According to FHWA (2019), more than 25 percent of fatal crashes were associated with horizontal curves, and about three-quarters of these fatal crashes were related to single vehicles leaving the roadway. Studies have shown that vehicle skidding is a key cause of lane/roadway departure crashes on horizontal curves, particularly in wet weather (Olsen, 1978; Xiao et al., 2000; Mayora and Piña, 2009). Studies also found that the crash rate in wet weather was significantly higher than that under dry conditions (Andrey and Yagar, 1993; Mayora and Piña, 2009; Geedipally et al., 2020). The aforementioned statistics and findings of past research provided the motivation for the present study to examine the mechanisms of vehicle skidding on wet horizontal curves. It is an objective of this study to provide useful information to researchers and practitioners in identifying the important factors that contribute to horizontal curve crashes.

This study analyzed three possible modes of vehicle skidding on

\* Corresponding author at: School of Highway, Chang'an University, China.

E-mail address: [ceefwatf@nus.edu.sg](mailto:ceefwatf@nus.edu.sg) (T.F. Fwa).

horizontal curves based on theories of mechanics. They were (i) forward skidding of front steering wheel, (ii) sideway skidding of front steering wheel, and (iii) sideway skidding of rear wheel. The skidding analysis was performed using a computer simulation model developed by the authors. It was based on the consideration of dynamic interaction of vehicle tyres, pavement surface properties and the thickness of water present on the pavement surface. The analysis would identify the states at which skidding would occur. A state refers to a combination of specific conditions of vehicle, horizontal curve, pavement, environment and weather. The results are presented in quantitative terms graphically for easy reference.

## 2. Review of past studies of crashes on horizontal crashes

Research efforts studying driving safety and crash reduction on horizontal curves can be broadly classified into two main approaches. The first approach aims to identify significant contributing factors to horizontal curve crashes and applies statistical techniques to develop predictive models for crashes. The second approach focuses on traffic and road related factors that could be managed by highway authorities and management agencies, and recommends measures implementable to reduce the risk of crashes. **Tables 1 and 2** are prepared based on a literature review conducted in this research based on related research studies reported in the last three decades. Though the review may not be exhaustive, it is believed that the information summarized in the two tables provides a fair representation of the general consensus on the important factors contributing to crashes on horizontal curves.

In **Table 1**, the contributing factors found to be statistically significant by studies in the first approach are grouped into the following four main categories: (i) Roadway curve geometric characteristics, (ii) Traffic flow characteristics, (iii) Pavement conditions, and (iv) Environmental factors. One or more curve geometric characteristics were identified by all studies as significant contributing factors. All but one studies found traffic volume to be an important contributing factor. Vehicle speed was

found significant in only two studies. In the last two categories, i.e. pavement and environmental factors, only three and two studies respectively found them to be statistically significant. It should be noted that each empty cells in **Table 1** means that the factor concerned was either (i) not considered in the study at all, or (ii) found insignificant statistically. In most studies, reason (i) was the reason. This is understandable as data on vehicle speed, pavement condition and environmental factors are either incomplete or unavailable in many databases. Under "Other Factors" in the last column, with the exception of warning sign, all the significant factors identified were curve geometric characteristics related to design consistency.

**Table 2** lists the measures implemented and found effective in efforts to reduce crashes on horizontal curves. These measures are classified under four main categories: warning system, speed management, geometric design consistency, and pavement friction management. The first two are measures that aim to alert drivers to reduce their speeds on the understanding from past research and experience that lower speed would help to reduce crash risk. The third category of measures is more applicable to actions to be taken during the design phase, and is not common as a form of field treatment due to cost consideration. In comparison, the fourth category (i.e. pavement friction management) is the most common option employed by pavement management agencies.

There is a common feature of all the studies in the two approaches presented in **Tables 1 and 2**. It is that the relationships between the identified factors and crash rate were established by means statistical techniques based on reported data. Theoretically, a crash is a physical process which is a result of the dynamic interaction between the moving vehicle and the pavement surface concerned, under the influence of environmental factors there and then. An analysis of this physical process could offer insights into the interaction mechanism, and help to identify the key contributing factors of a crash. The following sections present such an analysis for the case of vehicle skidding, which is known to be a main cause of roadway/lane departure crashes on horizontal curves.

**Table 1**  
Significant contributing factors in statistical prediction models of horizontal-curve crashes.

References	Curve				Traffic		Pavement		Environment		Other Factors
	Radius	Length	Angle	Lane Width	AADT	Speed	Skid Value	Condition	Rainy Day	Darkness	
Zegeer et al. (1991)	✓	✓	✓	✓							Spiral transition
Fink and Krammes (1995)		✓									Tangent lengths; Sight distance
Milton and Manning (1996)	✓				✓	✓					Tangent lengths; Number of lanes
Persaud et al. (2000)	✓	✓				✓					
Montella (2009)	✓		✓			✓			✓		
Srinivasan et al. (2009)	✓					✓			✓		Warning sign
Lord et al. (2011)		✓	✓	✓	✓	✓					Shoulder width
De Oña and Garach (2012)		✓	✓	✓	✓	✓					
Bauer and Harwood (2013)	✓					✓					Grade
Hauer (2015)	✓			✓	✓	✓					Shoulder width
Pratt et al. (2014)	✓		✓	✓	✓	✓		✓			
Gooch et al. (2016)		✓	✓	✓		✓					Adjacent curves
Saleem and Persaud (2017)	✓	✓	✓			✓					
Geedipally and Pratt (2017)	✓			✓	✓	✓					Shoulder width
Donnell et al. (2019)	✓	✓		✓	✓	✓		✓			Grade; Adjacent curves; Tangent lengths; Warning sign
Dhahir and Hassan (2019)		✓				✓					Speed reduction**; Speed limit*
Xin et al. (2019)	✓	✓	✓		✓	✓		✓			Grade; Auxiliary lane; Reverse curve
Ma et al. (2020)		✓			✓	✓					Speed limit*; Elevation fluctuation

Notes: \* Posted speed limit.

\*\* Reduction in the 85th percentile speeds of tangent and curve segments.

**Table 2**

Effective measures in studies for reducing crashes on horizontal curves.

Category	Reference	Description of Crash Reduction Measure
1. Warning system	Montella (2009)	Chevron signs, curve warning signs, flashing beacons
	Srinivasan et al. (2009)	Advance warning signs; fluorescent signs
	Ré et al. (2010)	Chevrons with retroreflective signposts
2. Speed management	Charlton (2007)	Chevron signs, advance warning signs, pavement markings, rumble strips
	Donnell et al. (2019)	Guiderail with delineator.
	Wood and Donnell (2020)	On-pavement warning marking ahead of horizontal curves.
	Cruzado and Donnell (2009)	Dynamic speed display signs
	Gehlert et al. (2012)	Dynamic speed display signs
	Hallmark et al. (2015)	Dynamic speed feedback signs
	Dhahir and Hassan (2019)	Curve speed reduction
3. Geometric design consistency	Donnell et al. (2019)	Characteristics of upstream tangent, upstream horizontal curve, downstream tangent, and downstream horizontal curve.
	Sinhal (2005)	Pavement skid resistance threshold value
	Mayora and Piña (2009)	Lateral friction of pavement
4. Pavement condition improvement	Schram (2011)	Minimum pavement friction threshold
	Buddhavarapu et al. (2013)	Pavement distress condition; pavement roughness index
	Musey and Park (2016)	High friction surface treatment
	Donnell et al. (2019)	Lateral friction improvement

### 3. Vehicle skidding modes on wet horizontal curves

The turning motion of a vehicle traveling on a horizontal curve involves continuous adjustments of the direction of movement. This is achieved through controlling the front steering wheels to maintain an appropriate yaw angle (i.e. slip angle) between the direction of vehicle movement and the longitudinal axis of the steering wheels. Because of the turning movement, both the front and rear wheels of the vehicle would experience centrifugal forces in the radial direction, in addition to the usual forces associated with the forward movement of the vehicle. These are the forces to be considered in vehicle skidding analysis.

Based on past research studies on vehicle skidding (Bergman, 1977; Ryu et al., 2013; Anupam et al., 2014; Peng et al., 2020), the following three possible vehicle skidding modes were considered in the present study: (i) Mode 1 – Forward skidding of front steering wheel, (ii) Mode 2 – Sideway skidding of front steering wheel, and (iii) Mode 3 – Sideway skidding of rear wheel. Fig. 1 shows schematically the three modes of wheel skidding for a vehicle traveling on a horizontal curve. Mode 1 is not the same as the forward skidding of a vehicle moving on a straight road section. The main difference is the presence of a yaw angle (i.e. slip angle) associated with the vehicle turning movement on the curve. This is a possible skidding mode because the forward tyre-pavement skid resistance would decrease as the magnitude of the slip angle increases. Skid resistance is a term used in pavement engineering to refer to the maximum resisting force that can be generated at a tyre-pavement interface when a tyre slides on the pavement surface. Skidding of a tyre occurs on a pavement when its skid resistance demand exceeds the tyre-pavement skid resistance.

Mode 2 and Mode 3 skidding occur under the action of centrifugal

force generated from the circular movement of a vehicle moving on a horizontal curve. This tendency to skid outward in the direction perpendicular to the vehicle movement trajectory is resisted by tyre-pavement skid resistance in the direction of skidding. The two modes of skidding are not exactly the same because in the circular motion of a vehicle, the slip angles of the front and rear wheels are different. Another factor that could contribute to different skidding behaviors of the front and rear wheels is the likely difference between their wheel loads.

Skidding of a vehicle would occur when the friction demand of the vehicle's turning movement exceeds the skid resistance that can be generated from the tyre-pavement interface. The friction demand of a vehicle increases as its speed increases. The term "skidding potential" is defined in this study as the difference between the traveling speed of a vehicle and the maximum safe speed against skidding. The smaller the difference, the higher is the skidding potential. According to past research on vehicle skidding, the magnitude of tyre-pavement skid resistance available is dependent on the properties of tyre and pavement surface, the geometric characteristics of the curve, and other external factors such as the thickness of water film on the pavement surface. The relative contributions of each of these factors are examined in the following sections through a mechanics-based finite element analysis of their dynamic interaction.

### 4. Development and validation of finite-element skid resistance simulation model

#### 4.1. Development of finite-element skid resistance simulation model

The simulation model developed and validated by the authors in their earlier work (Peng et al., 2020) was adopted in the present study. This earlier work by Peng et al. (2020) focused on design speed determination for engineering design of new highway horizontal curves, based on a known design skid resistance value. In the present study, instead of designing new horizontal curve pavements, the focus is to study vehicle skidding potential on in-service pavement curves by determining the unknown pavement skid resistance. The simulation model would be applied to analyze the effects of different contributing factors on the magnitude of available tyre-pavement skid resistance under different operating conditions of a vehicle traveling on a horizontal curve.

Fig. 2 offers a simple explanation to the wet-pavement skid resistance simulation analysis of the finite element model adopted. It shows a schematic representation of the dynamic interaction of tyre, water and pavement surface when a vehicle moves on a wet pavement. For a rolling tyre to generate friction from a wet pavement, it must first displace the surface water from the pavement surface. Depending on the vehicle speed, not all the water may be replaced in time before the tyre rolls forward. That is, the magnitude of tyre-pavement contact area necessary for friction generation is dependent on the vehicle speed. The higher the vehicle speed, the smaller is the contact area, and the lower the magnitude of tyre-pavement friction generated. The reduction in tyre-pavement contact area, plus the fact that the tyre-pavement friction of a pavement when wetted is usually lower than when it is dry by a good margin, explain why the tyre-pavement skid resistance under a moving tyre can be substantially lower in wet-weather than on a dry day.

Although the detailed analysis involved in finite element computer simulation is much more complicated than that described in the preceding paragraph, the basic mechanism of skid resistance generation remains the same. The actual analysis involves calculation of the instantaneous hydrodynamic pressure developed, and the deformation and vibration modes of the tyre resulted from dynamic interaction among tyre, water and pavement surface. The analysis is performed using the theories of solid mechanics and hydrodynamics. The main components of the simulation modeling consist of development of the

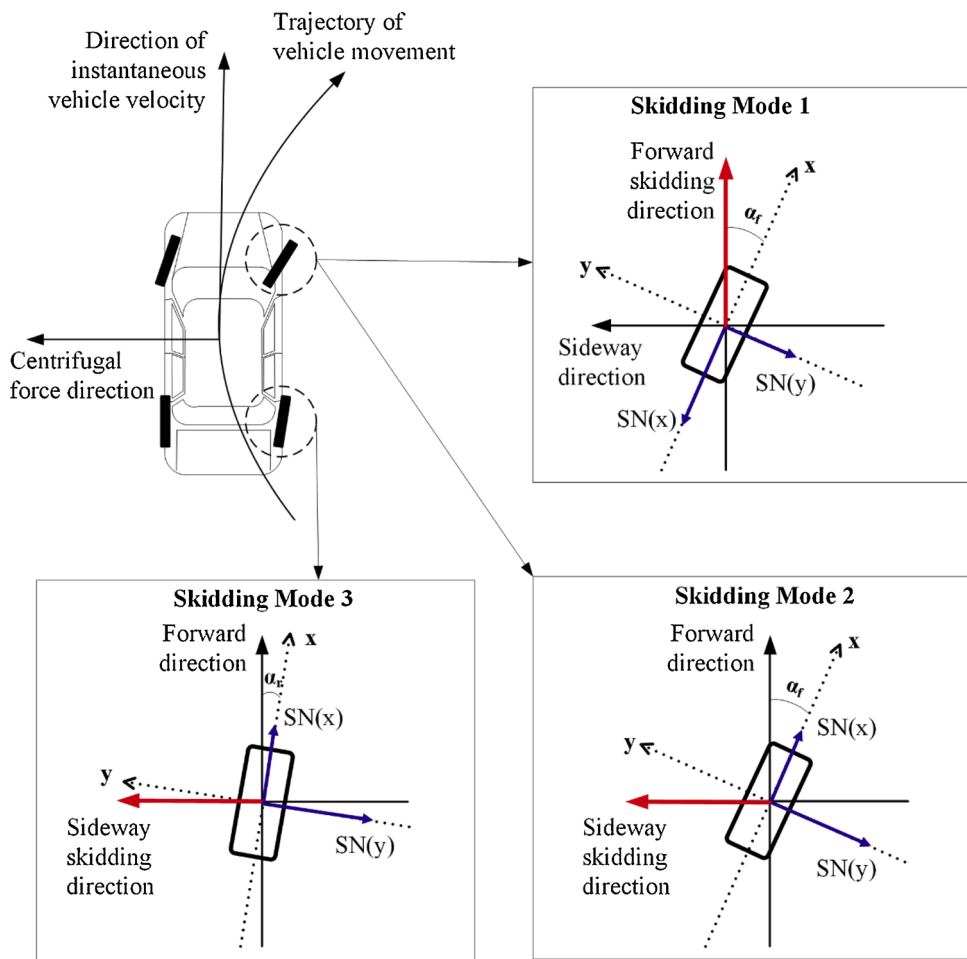


**Fig. 1.** Schematic representation of vehicle skidding modes considered.

Note:  $\alpha_f$  and  $\alpha_r$  are respectively the front and rear wheel slip angles when the vehicle is turning a corner.

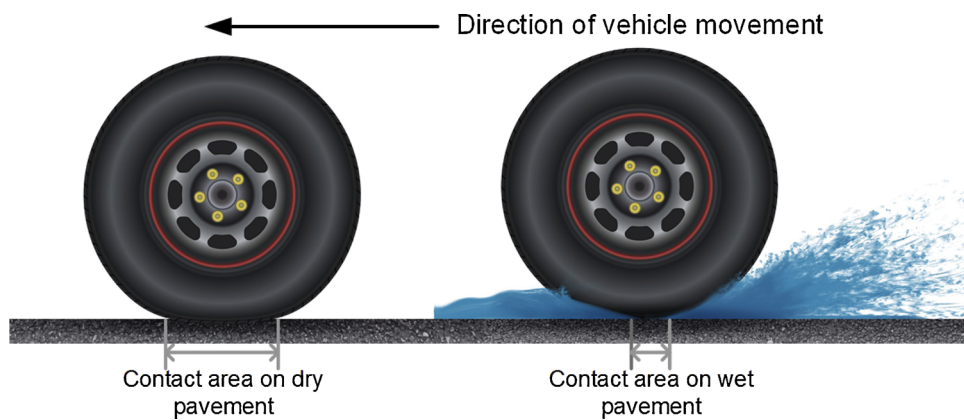


**Fig. 2.** Simplified schematic representation of tire-water-pavement interaction.

tire sub-model, water and pavement sub-models, and dynamic tire-fluid-pavement interaction analysis. The pavement surface is assumed to be ideally rigid and modeled using discrete rigid elements. The Coupled Eulerian-Lagrangian (CEL) method was applied to simulate the Eulerian-Lagrangian contact between fluid and tire structure. Fig. 3 shows an overview of the finite-element mesh used in the analysis of the three modes of skidding studied.

In Mode 1 skidding, the relative movement direction of the tyre and water is at a yaw angle  $\alpha$  with the longitudinal axis of the tyre. In Mode 2

and Mode 3 skidding, the relative movement take place in the radial direction of the horizontal curve. Table 3 lists the input parameters required for the analysis, as well as the output from the analysis. The input parameters are grouped under four categories: (i) Horizontal curve parameters, (ii) Pavement parameters, (iii) Vehicle parameters, and (iv) Environmental parameters. For a given horizontal curve, the values of the parameters in the first two categories can be obtained from on-site measurements. The last two categories are the vehicle operating variables that have to be carefully assessed. For example, either a

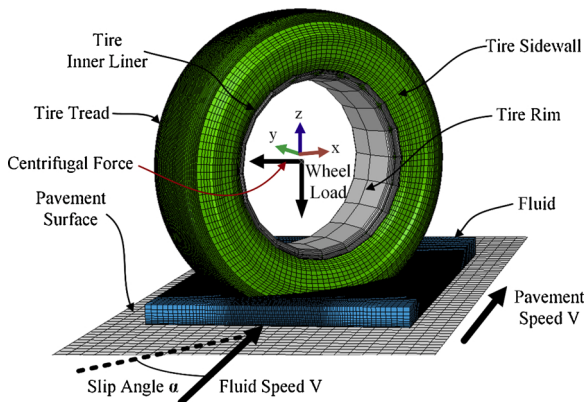


Fig. 3. Finite element models for skidding analysis.

**Table 3**  
Input and output parameters of finite element skidding analysis.

Input	Output
Horizontal Curve Parameters	Curve radius
	Superelevation rate
	Longitudinal grade
	Surface microtexture
Pavement Parameters	Surface macrotexture
	Permeability coefficient
	Tire type and dimensions
	Tire structural properties
Vehicle Parameters	Tire inflation pressure
	Wheel load
	Tire slip ratio
	Tire slip angle
Environmental Parameters	Vehicle speed
	Water film thickness
	Water temperature
	Air temperature
Energy dissipation	

representative vehicle type or a selected number of vehicle types, and an appropriate vehicle speed may be considered for the analysis. Representative vehicle types are selected by first identifying the main vehicle classes in the volume composition of the horizontal-curve traffic. A typical vehicle type in each vehicle class is next identified and considered in the simulation analysis to calculate the maximum safe speed against skidding for this vehicle type. The maximum safe speeds against skidding for different vehicle types are likely to be different because of their differences in wheel loads and tire properties.

For the water film thickness in the category of environmental parameters, it is appropriate to consider a range of water film thickness values corresponding to the rainfall intensities expected for the location of analysis. The thicker the water film on a pavement surface, the lower would be the skid resistance generated under a tire moving at a given speed. This is because the tire-pavement contact area at a given vehicle speed would decrease as the water film thickness becomes thicker. This means that all things being equal, the skidding potential of a moving vehicle would increase with water film thickness.

#### 4.2. Validation of finite-element skid resistance simulation model

The finite-element pavement skid resistance simulation technique was first applied in the last decade to solve the tyre-water-pavement interaction problem for the determination of tyre-pavement skid resistance on a wet pavement (Ong and Fwa, 2007). It has now been widely employed by researchers to study a wide range of skid resistance problems for different pavement designs under various forms of vehicle

operating conditions, using commercial finite element software such as ABAQUS, ANSYS and ADINA (Ong and Fwa, 2007; Zhang et al., 2013; Srirangam et al., 2014; Peng et al., 2020). These research studies provided validation of finite-element skid resistance simulation using field measured skid resistance data for different wet pavement conditions. They have confirmed the finite-element approach as a theoretically rigorous and reliable analytical tool to solve pavement-fluid interaction problems for the determination of pavement skid resistance.

The research studies mentioned in the preceding paragraph analyzed tyre-pavement skid resistance problems of straight road sections. Using the same theoretical approach, Peng et al. (2020) developed a finite-element simulation model for studying tyre-pavement skid resistance of horizontal-curve pavements. To demonstrate that the model was able to simulate the turning movements of a vehicle on horizontal curves, Peng et al. validated their model for Mode 1, 2 and 3 skid resistance using experimentally measured data for slip angles ranging from 0 to 90 degrees. This model is adopted for the present study.

To provide further confirmation that this model is applicable for the present study, another validation is provided here based on the field data measured in an experimental study by Horne (1969). The experiment was conducted on a concrete pavement lane with a radius of 500 ft (152.4 m). Table 4(a) presents the validation data of tyre footprint dimensions which define the initial contact area between the deformed tyre and the pavement surface. As shown in Table 4(b), the experiment measured Mode 1 skid resistance at two slip ratios and three vehicle speeds for the water depth of 5 mm. The table compares the measured and model predicted skid resistance for each of the six test conditions. The results indicate that the simulation model is able to produce skid resistance with errors within practically acceptable limits. The results of this validation provide a further confirmation of the applicability of the finite-element simulation model for the present study. Fig. 4 presents images from the computer simulation showing the progressive changes of tire-pavement contact area as vehicles speed increases. Fig. 5 plots the changes of the following three forces as vehicle speed increases: the fluid uplift force acting on the tyre, the normal contact force at the tyre-pavement interface, and the tyre-pavement friction force.

## 5. Numerical example illustrating impacts of factors on skidding

### 5.1. Problem description

To illustrate the manners that different parameters interact to influence the skidding behavior of a two-axle passenger car, the finite element simulation model of ASTM E524 standard tire (ASTM E524-08, 2020) was applied to analyze a numerical example problem with the following selected values of input parameters:

- (a) Curve parameters – Curve radius: R = 100, 200 and 300 m;  
Superelevation: e = 2, 4, 6, 8 and 10 %
- (b) Pavement parameters – Skid resistance state 1: SN<sub>0</sub> = 73, SN<sub>64</sub> = 40;  
Skid resistance state 2: SN<sub>0</sub> = 60, SN<sub>64</sub> = 37  
(Note: SN<sub>0</sub> is the zero-speed skid number and SN<sub>64</sub> is the skid number measured at 64 km/h according to ASTM E274 standard procedure.)
- (c) Vehicle parameters – Front tyre: Slip angle = 13°, Load = 5.2 kN, Pressure = 165.5 kPa;  
Rear tyre: Slip angle = 4°, Load = 4.5 kN, Pressure = 165.5 kPa  
Speed: 40, 60, 80, 100 km/h  
Slip ratio: 15 %
- (d) Environment parameters – Water film thickness: 0, 1.0 and 2.5 mm;  
Air temperature: 25°C

Two classes of input parameters can be identified from the above list. They are: (i) the main input variables each of which was assigned a

**Table 4**

Comparison of experimental measured data and model predicted value.

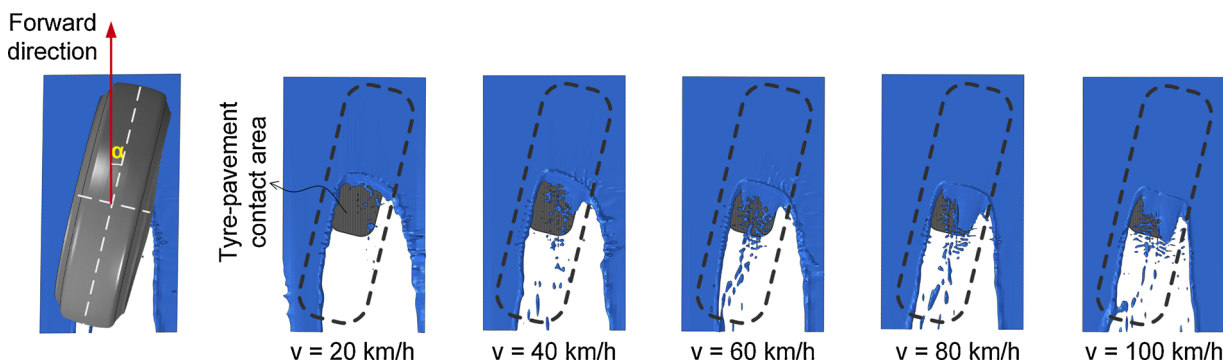
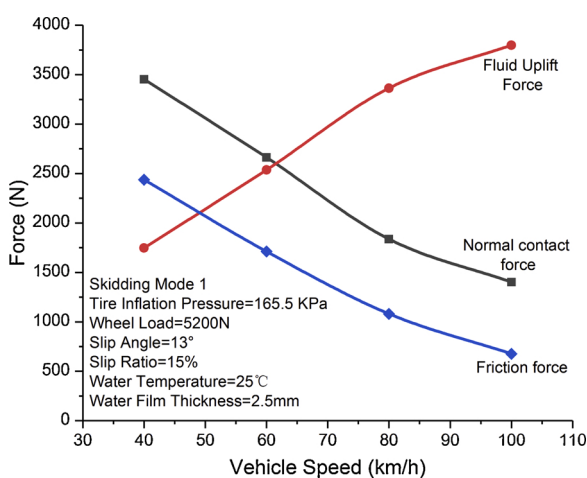
Wheel Load(N)	Footprint Length			Footprint Width		
	Measured (mm)	Simulated (mm)	Error (%)	Measured (mm)	Simulated (mm)	Error (%)
2200	120	112	-6.67	143	135	-5.59
3400	148	140	-5.41	145	140	-3.45
4600	176	164	-6.82	146	142	-2.74
5800	203	186	-8.37	147	142	-3.40

(b) Comparison of measured and model predicted skid resistance							
Type of texture	Water depth (mm)	Slip ratio (%)	Speed (km/h)	Measured skid number (SN)	Predicted Skid Number (SN)	Numerical difference	Error (%)
concrete curve lane (Horne, 1969)	5	100	16	25	24.92	-0.08	-0.32
			32	14	14.26	0.26	1.86
			48	10	10.47	0.47	4.70
		15	16	48	47.80	-0.20	-0.42
			32	40	39.78	-0.22	-0.55
			48	24	24.58	0.58	2.42

Note: Tyre model was ASTM E524 tyre (ASTM E524-08, 2020) with an inflation pressure of 165 KPa.

Note: Forward skid resistance value = ratio of tyre-pavement friction force and wheel load. SN = skid resistance value multiplied by 100.

**Fig. 4.** Graphical output of changes of tyre-pavement contact area as vehicle speed increases.**Fig. 5.** Variation of normal tyre-pavement contact force, fluid uplift force and tyre-pavement friction force with vehicle speed.

range of values to study their impacts on the skid resistance, and (ii) the secondary input parameters with a fixed value assigned to each. The main input variables are those parameters known to have significant effects on the magnitude of tyre-pavement skid resistance. They include curve radius, curve superelevation, pavement skid resistance state, vehicle speed and water film thickness. Among these parameters, curve radius and superelevation are chosen from within the common range

recommended by AASHTO (2018).

Pavement skid resistance state describes the surface characteristics of the pavement that, through interaction with the vehicle tyre and water on the pavement surface, govern the magnitude of skid resistance that can be generated between the tyre and the pavement (Fwa and Chu, 2019). Pavement surface microtexture and macrotexture are the two governing pavement characteristics widely adopted in pavement engineering for the purpose of skid resistance study (Leu and Henry, 1983; Henry, 2000; Fwa and Chu, 2019). In the concept of pavement skid resistance state,  $SN_0$  represents the effect of microtexture, and the effect of macrotexture is represented by  $SN_0$  and  $SN_{64}$  together (Chu and Fwa, 2016; Fwa and Chu, 2019). Two skid resistance states were considered for the purpose of assessing the effect of pavement skid resistance deterioration on skidding potential. This serves to highlight the fact that, under the effect of traffic action, the skid resistance of all in-service pavements would decrease with time until a stable terminal state. Hence, for a given horizontal curve pavement section, all other conditions remain constant, the skidding potential of vehicles would increase over time as the pavement ages. It is also appropriate to stress that the rate of deterioration of a pavement is a function of the properties of the pavement surface material. For example, the skid resistance characteristics of an asphalt pavement are different from those of a concrete pavement. They are also different between different asphalt materials, or different concrete materials.

Fixed values were assigned to the following secondary input parameters: Tyre slip angle, tire load, tyre inflation pressure, and air temperature. When a vehicle negotiates a horizontal curve at a given speed, the slip angle of the front steering tyres tend to be larger on a

curve with a larger curvature (i.e. smaller radius). However, within the usual range of curve radius design and constructed according to standard practices, the slip angle would vary within a rather small range of  $0^\circ$  to  $16^\circ$ , and is less than about  $13^\circ$  for practically all normal vehicle operations (Cheli et al., 2007; Melzi and Sabbioni, 2011; Ryu et al., 2013; Naets et al., 2017; Todoru and Cordon, 2018; Singh, 2019). Although the value of tyre-pavement skid resistance would generally decrease as the slip angle increases, its variation within the range of slip angle mentioned is of the order of about 1% (Bergman, 1977; Peng et al., 2020). Hence, the fixed values of  $13^\circ$  and  $4^\circ$  were used for the front and rear tyres respectively to represent their likely critical conditions for skidding potential analysis.

The tyre loads of 5.2 kN for each front tyre and 4.5 kN for each rear tyre, and the tyre pressure of 165.5 kPa are typical values for a representative passenger car. Past experimental and theoretical studies have shown that tyre-pavement skid resistance varies positively with tyre load and tyre pressure (Sacia, 1976; Gallaway et al., 1979; Ong and Fwa, 2010). That is, tyre-pavement skid resistance decreases as the magnitude of tyre load falls and the tyre pressure reduces. These studies also revealed that the impacts of tyre load and tyre pressure were much less significant than the main input parameters identified earlier. Since the tyre loads and pressures of passenger cars vary over rather narrow ranges compared with trucks and buses, constant values were assigned for both in the example problem.

### 5.2. Results of simulation – effects of factors on available skid resistance

The results of simulation analysis are plotted in Figs. 6–8 for skidding mode 1, 2 and 3 respectively. In the figures, each curve that links 4 data points, known as a skid resistance curve, gives the maximum available tyre-pavement skid resistance under the stated vehicle operating conditions and water film thickness. The curves in solid lines refer to available skid resistance for the pavement in skid resistance state 1, while those in dashed lines represent the case when the skid resistance state of the pavement deteriorates to state 2. These results in these figures showed that the available skid resistance on a wet pavement is affected by different factors in the following ways:

- The available skid resistance decreases as vehicle speed increases.
- The available skid resistance decreases as water depth (i.e. water film thickness) increases.
- The available skid resistance decreases as the pavement skid resistance state deteriorates.

### 5.3. Results of simulation – effects of factors on skid resistance demand

There are three sets of faint dotted curves each in Figs. 7 and 8. Each

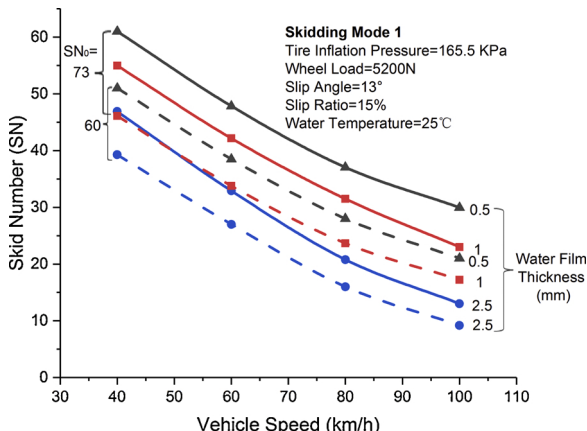


Fig. 6. The results of simulation analysis for skidding mode 1.

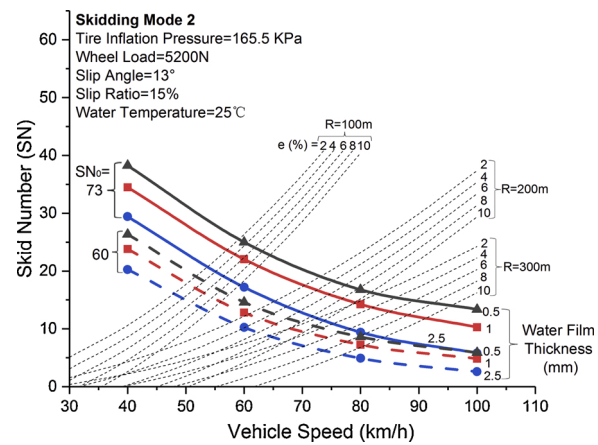


Fig. 7. The results of simulation analysis for skidding mode 2.

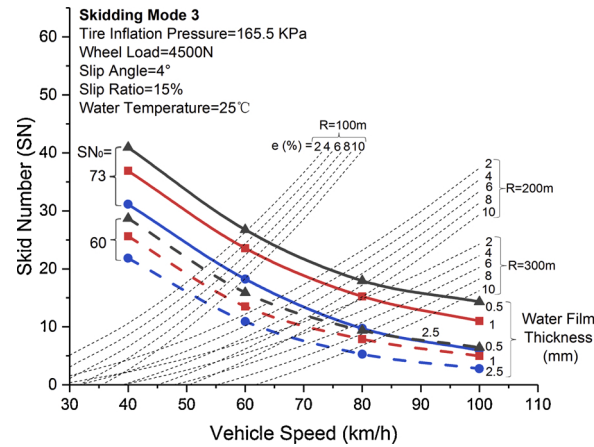


Fig. 8. The results of simulation analysis for skidding mode 3.

set represents the skid resistance demand, i.e. the minimum tyre-pavement skid resistance required to prevent skidding, for the stated curve radius  $R$  and superelevation  $e$ . Each of these curve gives the skid resistance demand as a function of vehicle speed for the given  $R$  and  $e$ . Skid resistance demand is the magnitude of skid resistance needed to prevent skidding caused by the centrifugal force of curve movement of the vehicle. Skidding occurs when the skid resistance demand exceeds the available tyre-pavement skid resistance. Hence, in Figs. 7 and 8, an intersection point of a skid resistance demand curve (a faint dotted curve) and an available skid resistance curve (either a solid or dashed line curve) gives the maximum safe speed for the indicated  $R$  and  $e$ . The skid resistance demand  $SN_d$  can be calculated based on Newtonian mechanics as follows:

$$SN_d = 100 \left( \frac{V^2}{gR} - \frac{e}{100} \right) \quad (1)$$

Where  $V$  is the vehicle speed of the traffic stream,  $R$  the curve radius,  $g$  the gravitational acceleration, and  $e$  the superelevation in percent. The skid resistance demand is a function of the square of vehicle speed. At a given vehicle speed, its magnitude decreases as the curve radius and the superelevation increase.

For skid resistance mode 1 shown in Fig. 6, the effects of curve radius and superelevation on the available tyre-pavement skid resistance for skidding mode 1 is practically negligible. This is because the difference in tyre slip angle is very small for the normal range of curve radii. Hence the skid resistance demand curves are not shown in Fig. 6. Past studies have shown that during a cornering movement, the longitudinal tire force is much smaller than the lateral tire force (Wang et al., 2014). In

other words, the skid resistance demand of the front wheels is governed by that of skidding mode 2.

#### 5.4. Results of simulation – critical skidding mode and influencing factors

**Fig. 9(a)** and (b) plot the available tyre-pavement skid resistance curves for the three skidding modes together for skid resistance state 1 and 2 respectively. From the discussion in preceding sections, it is apparent that the two radial skidding modes (i.e. skidding modes 2 and 3) present the most critical skidding potential. By comparing the available skid resistance with the skid resistance demand as presented in **Figs. 7 and 8**, it is obtained as presented in **Table 5** the maximum safe vehicle speeds for different combinations of curve radius R, superelevation e, water film thickness, and skid resistance state represented by  $SN_0$ . In general, all factors being equal, the skidding potential of a vehicle is higher under a condition when the maximum safe vehicle speed is lower. Hence, from the results in **Table 5**, the influence of individual factors on skidding potential can be stated as follows when all other factors are held constant:

- |                                 |  |
|---------------------------------|--|
| Skidding potential increases as | <ul style="list-style-type: none"> <li>(i) Vehicle speed V increases; or</li> <li>(ii) Curve radius R reduces; or</li> <li>(iii) Superelevation e decreases; or</li> <li>(iv) Water film thickness W increases; or</li> <li>(v) Pavement skid resistance deteriorates (i.e. lower <math>SN_0</math>).</li> </ul> |
|---------------------------------|--|

In reality, the exact evaluation of the skidding potential of a vehicle

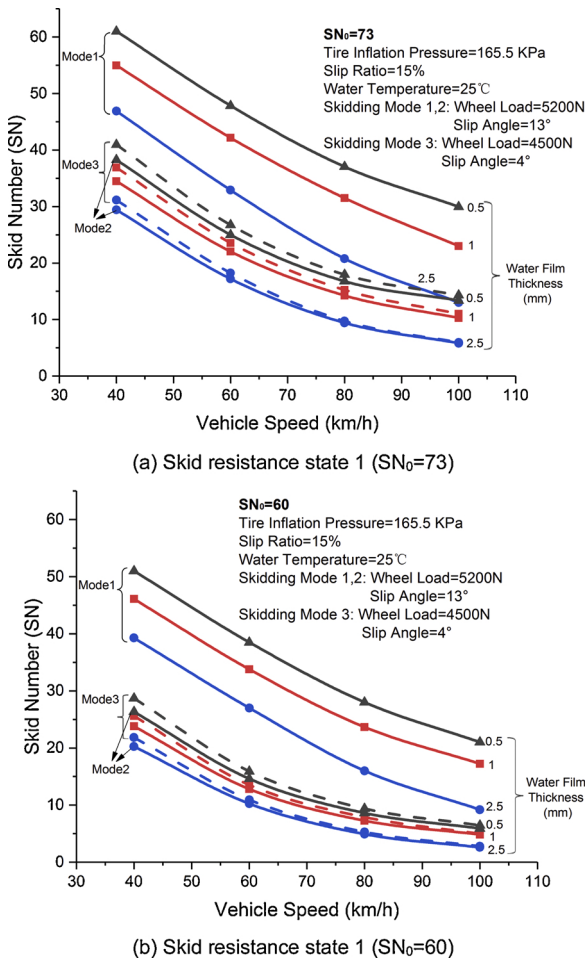


**Fig. 9.** Comparison of the available tyre-pavement skid resistance curves for the three skidding modes for skid resistance state 1 and 2.

negotiating a horizontal curve is a complex matter. While the two geometric factors  $R$  and  $e$  are constant for a known horizontal curve, the other three factors  $V$ ,  $W$  and  $SN_0$  are not. Vehicle speed is a driver's choice and it typically varies from one vehicle to another. Water film thickness is a function of weather condition and surface characteristics of pavement material. Pavement skid resistance state deteriorates with time under traffic abrasive actions. Eventually, it is the interaction of all these varying factors that determines the actual maximum safe vehicle speed. That is, the maximum safe speed of a known horizontal curve is a variable itself, with its value varying with time due to changes in environmental and pavement conditions.

The varying nature of some of the influencing factors has contributed to the difficulty in predicting the crash rate of a horizontal curve. For example, for a given horizontal curve, vehicle traveling at a specific speed could be safe in one period but not in another period, because of different pavement properties or climatic conditions. For the same reasons, two horizontal curves having identical geometric characteristics could have very different crash statistics. Furthermore, it should be noted that the maximum safe speed against skidding in **Table 5** apply to a specific set of tire properties, including tyre dimensions, tyre load and pressure, and rubber properties. It is possible that different vehicles traveling at the same speed on a horizontal curve could have different crash potential levels due to differences in their tire properties.

**Table 5** also lists the AASHTO design speeds (AASHTO, 2018) for comparison with the model calculated maximum safe speeds against skidding. The comparison shows that the AASHTO design speeds are safe for normal highway operating conditions with  $SN_0 = 0.73$  when  $w = 0$  mm (i.e. dry weather condition) and mild wet weather conditions when  $w = 0.5\text{--}1.0$  mm. AASHTO design speeds only become deficient for high-speed travel in severe wet-weather conditions. Driving at design speed in severe wet weather is not considered a normal operating condition since it is unsafe due to poor visibility, inadequate sight distance and low skid resistance. This consideration is in line with the fact that crashes are rare events, and it is an accepted practice that an engineering design cannot cater for all rare events.

The above-mentioned issues offer partial explanation to the differences among the crash rate prediction models obtained by statistics-based approaches shown in **Table 1**. One or more of the six key factors identified in this section were not included in all the studies. None considered any quantitative representation of pavement surface wetness (e.g. water film thickness). The two studies that included vehicle speed did not identify the actual speeds of vehicles involved in the crashes recorded – one considered posted speed limit, and the other considered reduction in the 85th percentile speeds of tangent and curve segments.

In **Table 2**, those studies in the other approach that evaluated the effectiveness of crash reduction measures focused on the following three aspects: (a) Signs or other information systems that alert drive to slow down (category 1 and 2), (b) Design consistency to reduce speed differential between tangent and curve segments (category 3), and (c) Pavement friction management to improve pavement skid resistance (category 4). Aspects (a) and (b) address the speed issue, while aspect (c) represents treatments to raise pavement skid resistance and hence reduce skidding potential. Measures in category (1) and (2) can be enhanced if up-to-date information on the varying maximum safe vehicle speed is available. Measures in category (4) can be improved if the knowledge of the skid resistance demand and the tyre-pavement skid resistance for different speeds and water film thicknesses can be determined.

All the uncertainties and difficulties identified above arise from the lack of information on the three factors: vehicle speed  $V$ , water-film thickness  $W$  and pavement skid resistance state  $SN_0$ . Today, these difficulties can be overcome relatively easily. Real-time capturing and recording of individual vehicle speeds is no longer an issue using laser technology. Pavement skid resistance state is also readily available in the pavement management system database of a highway agency because traffic-speed skid resistance testers has become a standard asset

**Table 5**

Calculated maximum safe vehicle speeds against skidding for different combinations of curve radius, superelevation, water film thickness, and skid resistance state represented by  $SN_0$ .

Curve Radius (m)	e (%)	AASHTO design speed (km/h)	Calculated Maximum Safe Vehicle Speed against Skidding (km/h) (Skidding Mode 2)							
			$SN_0 = 73$				$SN_0 = 60$			
			w=0	w=0.5	w=1	w=2.5	w=0	w=0.5	w=1	w=2.5
100	2	52	68.51	59.09	56.99	53.59	56.87	51.40	49.84	47.57
	4	53	69.92	60.44	58.39	55.00	58.45	52.86	51.34	49.13
	6	55	71.31	61.79	59.78	56.40	60.02	54.33	52.85	50.68
	8	57	72.69	63.13	61.16	57.80	61.59	55.79	54.35	52.23
	10	59	74.07	64.47	62.54	59.20	63.14	57.26	55.85	53.78
200	2	66	90.58	73.12	70.34	65.22	73.01	62.74	60.73	57.72
	4	69	93.29	75.24	72.48	67.32	75.61	65.03	63.07	60.08
	6	73	96.12	77.38	74.64	69.44	78.21	67.35	65.44	62.47
	8	75	99.12	79.55	76.80	71.57	80.81	69.70	67.83	64.88
	10	78	102.34	81.73	78.98	73.72	83.41	72.07	70.25	67.31
300	2	78	117.74	82.84	79.24	72.54	85.46	70.26	67.89	64.15
	4	83	118.18	85.78	82.08	75.27	89.12	73.33	71.00	67.23
	6	85	118.62	88.81	84.97	78.05	92.80	76.48	74.20	70.37
	8	89	119.05	91.94	87.90	80.88	96.47	79.68	77.46	73.59
	10	94	119.47	95.17	90.88	83.78	100.12	82.94	80.78	76.87

Notes: e = superelevation rate, w = water film thickness on pavement surface (mm), shaded cells refer to those cases where the AASHTO design speed exceeds the corresponding calculated maximum safe vehicle speed.

in practically all state highway agencies (AASHTO, 2008; FHWA, 2017). Lastly, several computer programs are now available for calculation of water-film thickness from an input of rainfall intensity and pavement geometry (Zhang et al., 2016; Ressel et al., 2019). By including these three factors in studies of crash rates of horizontal curves (such as those in Tables 1 and 2), it is believed that there would be much improved consistency among prediction models derived for different horizontal curves.

## 6. Summary and conclusions

This paper has presented a mechanistic analysis of the mechanisms of the following three possible passenger-car skidding modes on horizontal curves: a tangent skidding mode of the front steering wheels, and two radial skidding modes one involving the front steering wheels and the other the rear wheels. It was found that the two radial skidding modes presented higher skidding potential than the tangent skidding mode of the front wheels. For the slip angles, tyre loads and inflation pressure considered, the front wheels were found to present marginally higher skidding potential than the rear wheels. It is possible that with a different set of slip angles, tyre load distribution and uneven water film thickness between the front and rear tyres, the skidding potential of the rear tyres could become more critical.

The analysis showed that the five key factors that affect the skidding potential of vehicles negotiating a horizontal curve were: vehicle speed, curve radius, superelevation, water film thickness and pavement skid resistance state. This study highlighted that the actual vehicle speed of a vehicle involved in a crash, the water film thickness and the pavement skid resistance state at the time of crash were typically not available in the historical database used in past studies. This has contributed to the inadequacy of the crash rate prediction models derived from studies conducted so far. With today's data acquisition techniques and sensor technology, the travel speeds of individual vehicles as well as the real-time water film thickness and existing pavement skid resistance state can be captured and recorded. The availability of such information would help to improve researchers' capability in assessing skidding risk and implementing effective measures to reduce crash rates of horizontal curves.

## Funding

This work was supported by Fundamental Research Funds for the Central Universities [grant number 300102219307].

## CRediT authorship contribution statement

**Jia Peng:** Software, Validation, Formal analysis, Data curation, Visualization, Writing - review & editing. **L. Chu:** Conceptualization, Methodology, Investigation, Software, Writing - original draft, Writing - review & editing. **Tangjie Wang:** Software, Formal analysis. **T.F. Fwa:** Conceptualization, Methodology, Writing - original draft, Writing - review & editing, Supervision, Project administration, Funding acquisition.

## Declaration of Competing Interest

The authors report no declarations of interest.

## References

- AASHTO, 2008. Guide for Pavement Friction. American Association of State Highway and Transportation Officials, Washington DC.
- AASHTO, 2018. A Policy on Geometric Design of Highways and Streets, 7th ed. American Association of State Highway and Transportation, Washington DC.
- Andrey, J., Yagar, S., 1993. A temporal analysis of rain-related crash risk. *Accid. Anal. Prev.* 25 (4), 465–472.
- Anupam, K., Srirangam, S.K., Scarpas, A., Kasbergen, C., Kane, M., 2014. Study of cornering maneuvers of a pneumatic tire on asphalt pavement surfaces using the finite element method. *Transp. Res. Rec.* 2457 (1), 129–139. <https://doi.org/10.3141/2457-14>.
- ASTM E524-08, 2020. Standard Specification for Standard Smooth Tire for Pavement Skid-Resistance Tests, 2020. ASTM International, West Conshohocken, PA. www.astm.org.
- Bauer, K.M., Harwood, D.W., 2013. Safety effects of horizontal curve and grade combinations on rural two-lane highways. *Transp. Res. Rec.* 2398 (1), 37–49.
- Bergman, W., 1977. Skid resistance properties of tires and their influence on vehicle control. *Transp. Res.* 621, 8–18.
- Buddhavarapu, P., Banerjee, A., Prozzi, J.A., 2013. Influence of pavement condition on horizontal curve safety. *Accid. Anal. Prev.* 52, 9–18.
- Charlton, S.G., 2007. The role of attention in horizontal curves: a comparison of advance warning, delineation, and road marking treatments. *Accid. Anal. Prev.* 39 (5), 873–885. <https://doi.org/10.1016/j.aap.2006.12.007>.

- Cheli, F., Sabbioni, E., Pesce, M., Melzi, S., 2007. A methodology for vehicle sideslip angle identification: comparison with experimental data. *Veh. Syst. Dyn.* 45 (6), 549–563. <https://doi.org/10.1080/00423110601059112>.
- Cruzado, I., Donnell, E.T., 2009. Evaluating effectiveness of dynamic speed display signs in transition zones of two-lane, rural highways in Pennsylvania. *Transp. Res. Rec. J. Transp. Res. Board* 2122 (1), 1–8. <https://doi.org/10.3141/2122-01>.
- De Ona, J., Garach, L., 2012. Accidents prediction model based on speed reduction on spanish two-lane rural highways. *Procedia Soc. Behav. Sci.* 53, 1010–1018. <https://doi.org/10.1016/j.sbspro.2012.09.950>.
- Dahir, B., Hassan, Y., 2019. Using horizontal curve speed reduction extracted from the naturalistic driving study to predict curve collision frequency. *Accid. Anal. Prev.* 123, 190–199.
- Donnell, E., Porter, R.J., Li, L., Hamilton, I., Himes, S., Wood, J., 2019. Reducing Roadway Departure Crashes at Horizontal Curve Sections on Two-lane Rural Highways. Report No. FHWA-SA-19-005. Federal Highway Administration, Washington D.C.
- FHWA, 2017. Friction Management Program [Access date: 8/25/2020]. [https://safety.fhwa.dot.gov/roadway\\_dept/pavement\\_friction/friction\\_management/](https://safety.fhwa.dot.gov/roadway_dept/pavement_friction/friction_management/).
- FHWA, 2019. Horizontal Curve Safety [Access date: 8/25/2020]. [https://safety.fhwa.dot.gov/roadway\\_dept/countermeasures/horcurves/](https://safety.fhwa.dot.gov/roadway_dept/countermeasures/horcurves/).
- FHWA, 2020. Roadway Departure Safety [Access date: 8/25/2020]. [https://safety.fhwa.dot.gov/roadway\\_dept/](https://safety.fhwa.dot.gov/roadway_dept/).
- Fink, K.L., Krammes, R.A., 1995. Tangent length and sight distance effects on accident rates at horizontal curves on rural two-lane highways. *Transp. Res. Rec.* 1500, 162–168.
- Fwa, T.F., Chu, L., 2019. The concept of pavement skid resistance state. *Road Mater. Pavement Des.* 1–20. <https://doi.org/10.1080/14680629.2019.1618366>.
- Gallaway, B.M., Ivey, D.L., Hayes, G.G., Ledbetter, W.G., Olson, R.M., Woods, D.L., Schiller, R.E., 1979. Pavement and Geometric Design Criteria for Minimizing Hydroplaning. Federal Highway Administration Report No. FHWA-RD-79-31.
- Geedipally, S.R., Pratt, M.P., 2017. Predicting the distribution of vehicle travel paths along horizontal curves. *J. Transp. Eng. Part A Syst.* 143 (7), 04017021. <https://doi.org/10.1061/jtepbs.0000049>.
- Geedipally, S.R., Das, S., Pratt, M.P., Lord, D., 2020. Determining skid resistance needs on horizontal curves for different levels of precipitation. *Transp. Res. Rec. J. Transp. Res. Board*, 036119812092933. <https://doi.org/10.1177/0361198120929334>.
- Gehlerl, T., Schulze, C., Schlag, B., 2012. Evaluation of different types of dynamic speed display signs. *Transp. Res. Part F Traff. Psychol. Behav.* 15 (6), 667–675. <https://doi.org/10.1016/j.trf.2012.07.004>.
- Glennon, J.C., Neuman, T.R., Leisch, J.E., 1985. Safety and Operational Considerations for Design of Rural Highway Curves. Report No. FHWA-RD-86-035. Federal Highway Administration, McLean, VA.
- Gooch, J.P., Gayah, V.V., Donnell, E.T., 2016. Quantifying the safety effects of horizontal curves on two-way, two-lane rural roads. *Accid. Anal. Prev.* 92, 71–81. <https://doi.org/10.1016/j.aap.2016.03.024>.
- Hallmark, S.I., Hawkins, N., Smadi, O., 2015. Evaluation of Dynamic Speed Feedback Signs on Curves: A National Demonstration Project. Report No. FHWA-HRT-14-020. Center for Transportation Research and Education, Iowa State University, Ames, IA.
- Hauer, E., 2015. The Art of Regression Modeling in Road Safety. Springer International Publishing, Switzerland. <https://doi.org/10.1007/978-3-319-12529-9>.
- Henry, J.J., 2000. Evaluation of Pavement Friction Characteristics – a Synthesis of Highway Practice. NCHRP Synthesis 291. National Cooperative Highway Research Program., Washington, DC.
- Horne, W.B., 1969. Results from studies of highway grooving and texturing at NASA wallop station. *Pavement Grooving and Traction Studies*, NASA SP-5073. National Aeronautics and Space Administration, Washington D.C., USA, pp. 425–464.
- Leu, M.C., Henry, J.J., 1983. Prediction of Skid Resistance as a Function of Speed from Pavement Texture. *Transportation Research Record*, No. 946. Transportation Research Board., Washington, DC.
- Lord, D., Brewer, M.A., Fitzpatrick, K., Geedipally, S.R., Peng, Y., 2011. Analysis of Roadway Departure Crashes on Two Lane Rural Roads in Texas (No. FHWA/TX-11-0-6031-1). Texas Transportation Institute.
- Ma, Q., Yang, H., Wang, Z., Xie, K., Yang, D., 2020. Modeling crash risk of horizontal curves using large-scale auto-extracted roadway geometry data. *Accid. Anal. Prev.* 144, 105669. <https://doi.org/10.1016/j.aap.2020.105669>.
- Mayora, J.M.P., Piña, R.J., 2009. An assessment of the skid resistance effect on traffic safety under wet-pavement conditions. *Accid. Anal. Prev.* 41 (4), 881–886. <https://doi.org/10.1016/j.aap.2009.05.004>.
- Melzi, S., Sabbioni, E., 2011. On the vehicle sideslip angle estimation through neural networks: numerical and experimental results. *Mech. Syst. Signal Process.* 25 (6), 2005–2019. <https://doi.org/10.1016/j.ymssp.2010.10.015>.
- Milton, J.C., Mannerling, F.L., 1996. The Relationship between Highway Geometries, Traffic Related Elements and Motor Vehicle Accidents. Final Research Report, WA-RD 403.1 Washington State Department of Transportation, Washington.
- Montella, A., 2009. Safety evaluation of curve delineation improvements. *Transp. Res. Rec. J. Transp. Res. Board* 2103 (1), 69–79. <https://doi.org/10.3141/2103-09>.
- Musey, K., Park, S., 2016. Pavement skid number and horizontal curve safety. *Procedia Eng.* 145, 828–835. <https://doi.org/10.1016/j.proeng.2016.04.108>.
- Naets, F., Van Aalst, S., Boulkroune, B., Ghouti, N.E., Desmet, W., 2017. Design and experimental validation of a stable two-stage estimator for automotive sideslip angle and tire parameters. *IEEE Trans. Veh. Technol.* PP (11), 1–1.
- Olsen, R.A., 1978. The driver as cause or victim in vehicle skidding accidents. *Accid. Anal. Prev.* 10 (1), 61–67. [https://doi.org/10.1016/0001-4575\(78\)90008-8](https://doi.org/10.1016/0001-4575(78)90008-8).
- Ong, G.P., Fwa, T.F., 2007. Wet-pavement hydroplaning risk and skid resistance: modeling. *J. Transp. Eng.* 133 (10), 590–598. [https://doi.org/10.1061/\(ASCE\)0733-947X\(2007\)133:10\(590\)](https://doi.org/10.1061/(ASCE)0733-947X(2007)133:10(590)).
- Ong, G.P., Fwa, T.F., 2010. Modeling skid resistance of commercial trucks on highways. *J. Transp. Eng.* 136 (6), 510–517.
- Peng, J., Chu, L., Fwa, T.F., 2020. Determination of safe vehicle speeds on wet horizontal pavement curves. *Road Mater. Pavement Des.* 1–13. <https://doi.org/10.1080/14680629.2020.1772350>.
- Persaud, B., Retting, R., Lyon, C., 2000. Guidelines for identification of hazardous highway curves. *Transp. Res. Rec. J. Transp. Res. Board* 1717, 14–18. <https://doi.org/10.3141/1717-03>.
- Pratt, M.P., Geedipally, S.R., Pike, A.M., Carlson, P.J., Celoza, A.M., Lord, D., 2014. Evaluating the Need for Surface Treatments to Reduce Crash Frequency on Horizontal Curves. Report No. 0-6714-S. Texas A&M Transportation Institute, College Station, Texas.
- Ré, J.M., Hawkins, H.G., Chrysler, S.T., 2010. Assessing benefits of chevrons with full retroreflective signposts on rural horizontal curves. *Transp. Res. Rec. J. Transp. Res. Board* 2149 (1), 30–36. <https://doi.org/10.3141/2149-04>.
- Ressel, W., Wolff, A., Alber, S., Rucker, I., 2019. Modelling and simulation of pavement drainage. *Int. J. Pavement Eng.* 20 (7), 801–810.
- Ryu, J., Nardi, F., Moshchuk, N., 2013. Vehicle Sideslip Angle Estimation and Experimental Validation, Volume 4A. Dynamics, Vibration and Control. <https://doi.org/10.1115/imece2013-64466>.
- Sacia, S.R., 1976. The Effect of Operating Conditions on the Skid Performance of Tires. *Transportation Research Record*, No. 621, pp. 126–135.
- Saleem, T., Persaud, B., 2017. Another look at the safety effects of horizontal curvaturer on rural two-lane highways. *Accid. Anal. Prev.* 106, 149–159. <https://doi.org/10.1016/j.aap.2017.04.001>.
- Schram, S., 2011. Specifications for aggregate frictional qualities in flexible pavements. *Transp. Res. Rec. J. Transp. Res. Board* 2209 (1), 18–25. <https://doi.org/10.3141/2209-03>.
- Singh, K.B., 2019. Vehicle sideslip angle estimation based on tire model adaptation. *Electronics* 8 (2), 199. <https://doi.org/10.3390/electronics8020199>.
- Sinhal, R., 2005. The implementation of a skid policy to provide the required friction demand on the main road network in the United Kingdom. International Conference on Surface Friction, Christchurch, New Zealand, Transit New Zealand, Wellington, 13pp.
- Srinivasan, R., Baek, J., Carter, D., Persaud, B., Lyon, C., Eccles, K., Gross, F., Lefler, N., 2009. Safety Evaluation of Improved Curve Delineation. Report No. FHWA-HRT-09-045. Federal Highway Administration, Washington, DC.
- Srirangam, S.K., Anupam, K., Scarpas, A., Kasbergen, C., Kane, M., 2014. Safety aspects of wet asphalt pavement surfaces through field and numerical modeling investigations. *Transp. Res. Rec.* 2446 (1), 37–51. <https://doi.org/10.3141/2446-05>.
- Stimpson, W.A., McGee, H.W., Kittelson, W.K., Ruddy, R.H., 1977. Field Evaluation of Selected Delineation Treatments for Two-lane Rural Highways. Report No. FHWA-RD-77-118. Federal Highway Administration, Washington D.C.
- Taylor, J.I., McGee, H.W., Sequin, E.L., Hostettler, R.S., 1972. Roadway Delineation Systems. NCHRP Report 130, Highway Research Board, Washington, D.C.
- Todorut, A., Cordoş, N., 2018. Evaluation of the vehicle sideslip angle according to different road conditions. *Proc. Autom. Eng.* 814–819. [https://doi.org/10.1007/978-3-319-94409-8\\_95](https://doi.org/10.1007/978-3-319-94409-8_95).
- Torbic, D.J., Harwood, D.W., Gilmore, D.K., 2004. NCHRP Report 500: Guidance for Implementation of the AASHTO Strategic Highway Safety Plan, Volume 7: A Guide for Reducing Collisions on Horizontal Curves. Transportation Research Board of the National Academies, Washington, DC.
- Wang, H., Al-Qadi, I.L., Stanciulessu, I., 2014. Effect of surface friction on tire–pavement contact stresses during vehicle maneuvering. *J. Eng. Mech.* 140 (4) <https://doi.org/10.1016/j.asce.jem.1943-7889.0000691>, 04014001.
- Wood, J., Donnell, E.T., 2020. Empirical Bayes before-after evaluation of horizontal curve warning pavement markings on two-lane rural highways in Pennsylvania. *Accid. Anal. Prev.* 146 (2020), 1–6. <https://doi.org/10.1016/j.aap.2020.105734>, 105734.
- Xiao, J., Kulakowski, B., El-Gindy, M., 2000. Prediction of risk of wet-pavement accidents: fuzzy logic model. *Transp. Res. Rec. J. Transp. Res. Board* 1717, 28–36. <https://doi.org/10.3141/1717-05>.
- Xin, C., Wang, Z., Lee, C., Lin, P.-S., Chen, T., Guo, R., Lu, Q., 2019. Development of crash modification factors of horizontal curve design features for single-motorcycle crashes on rural two-lane highways: a matched case-control study. *Accid. Anal. Prev.* 123, 51–59. <https://doi.org/10.1016/j.aap.2018.11.008>.
- Zegeer, C., Stewart, R., Reinfurt, D., Council, F., Neuman, T., Hamilton, E., Miller, T., Hunter, W., 1991. Cost-Effective Geometric Improvements for Safety Upgrading of Horizontal Curves. Report FHWA-R0-90-021. FHWA, U.S. Department of Transportation.
- Zhang, L., Ong, G.P., Fwa, T.F., 2013. Developing an analysis framework to quantify and compare skid resistance performance on porous and nonporous pavements. *Transp. Res. Rec. J. Transp. Res. Board* 2369 (1), 77–86. <https://doi.org/10.3141/2369-09>.
- Zhang, L., Fwa, T.F., Ong, G.P., Chu, L., 2016. Analyzing effect of roadway width on skid resistance of porous pavement. *Road Mater. Pavement Des.* 17 (1), 1–14.